

## The potential effect of ellagic acid on cisplatin-induced hepatorenal toxicity in male albino rats.

Hani M. Abdelsalam<sup>1\*</sup>, Abdelaziz A Diab<sup>1</sup>, Atef G Hussein<sup>2</sup>, Nourhan I Gomaa<sup>3</sup>, Josef A Aziz<sup>4</sup>

<sup>1</sup>Department of Zoology, Zagazig University, Zagazig, Egypt

<sup>2</sup>Department of Medical Biochemistry, Zagazig University, Zagazig, Egypt

<sup>3</sup>Department of Bioscience, Sinai University, North Sinai Governorate 16020, Egypt

<sup>4</sup>Department of Anatomy and Embryology, Zagazig University, Zagazig, Egypt

### Abstract

**Purpose:** Cisplatin (Cis) is a commonly used cancer treatment drug, particularly in breast cancer. Nevertheless, the side effects of Cis have an impact on other body systems. This study aims to investigate the therapeutic potential of Ellagic acid (Ell) to alleviate the side effects of Cis.

**Methods:** Forty male albino rats were randomly divided into four groups: the Control group, Cis group, Ell group, and Cis+Ell group. To evaluate neurotransmitters, biochemical estimations of liver function, urea, creatinine, BUN, and brain tissue homogenates were performed. The liver and kidney slices from all groups were processed for histopathological and immunohistochemical analyses.

**Results:** Our studies proved that Ell caused a significant improvement in the antioxidant enzymes, MDA level, and both liver and kidney functions and disturbance in GABA and glutamate levels in brain homogenates after the negative effects induced by Cis. Ell also reduced cleavage of caspase 3 and immunoreactivity of COX2 in the kidneys of Cis-treated rats, increased expression of antiapoptotic Bcl2 in and suppressed the expression of P53 in the hepatocytes, and reduced cleavage of caspase 3 and the immunoreactivity of COX2 in the kidney of Cis-treated rats.

**Conclusion:** Treatment with Ell can effectively mitigate the negative effects on liver, kidney and brain that are caused by the administration of Cis.

**Keywords:** Cisplatin, Ellagic acid, Hormonal assay, Hepatocytes.

**Abbreviations:** Cis: Cisplatin; Ell: Ellagic acid; ALT: Alanine Transferase; MDA: Malondialdehyde; SOD: Superoxide Dismutase; GSH: Glutathione; ROS: Reactive Oxygen Species.

Accepted on July 29, 2022

### Introduction

Cisplatin (Cis) is a potent platinum-based antineoplastic agent used to treat a variety of cancers, including solid tumors that have proven resistant to other treatments. Among the most common cancers treated with it are lymphoma and stomach, esophageal, pancreatic, bladder, head and neck, lung, ovarian, and testicular cancers [1]. Cis causes hepatic injury by activating inflammatory and oxidative stress pathways, as well as causing apoptosis and structural and functional abnormalities in the liver [2]. Because Cis is primarily processed by the kidneys and liver, it has been linked to hepatotoxicity and nephrotoxicity [3]. Cis-induced nephrotoxicity can range from mild, reversible structural changes in tubular epithelial cells that cause a variety of renal dysfunction (acute nephrotoxicity)

to potentially irreversible renal failure that leads to chronic and progressive renal insufficiency (chronic and progressive renal insufficiency) (chronic nephrotoxicity) [4].

Ellagic acid (Ell) is a polyphenolic substance found in nuts, fruits, and vegetables [5]. Ell has antioxidant and anti-inflammatory activities [6,7]. Ell protects hepatocytes from Cis-induced damage by acting as a ROS scavenger and maintaining antioxidant enzyme levels [8]. However, it is unknown if Ell effects are mediated by Nrf2 activation and/or whether this antioxidant affects mitochondrial dysfunction, which is linked to Cis-induced hepatotoxicity [9]. Ell is a polyphenol found in plants that have antioxidative properties *in vivo* [10] and *in vitro* [11]. Ell is an effective scavenger of both ROS and lipid

peroxidation [12]. Furthermore, Ell therapy protects against Cis-induced nephrotoxicity while also lowering plasma creatinine and urea levels [13].

## **Materials and Methods**

### **Chemicals**

Acros organics in the USA provided cisplatin (250 mg, trace metal basis, code 193762500).

Acros organics in the USA also supplied 97% ellagic acid (2.5GR, code 117740025).

### **Animals and experimental design**

In this study, 40 healthy male adult albino rats weighing 150–180 g were used. The animals were obtained from Theodor Bilharz Research Institute, Cairo, Egypt and kept under normal conditions with free access to food and water. All animals were housed in hygienic plastic cages in well-ventilated rooms with exhaust fans; they were fed a standard pellet diet and had free access to water daily. All animal procedures were carried out with the approval of the Ethics Committee of the National Research Center, Egypt, and following recommendations of the institutional animal care and use committee of the Zagazig University (ZU-IACUC/3/f/21/2021). The rats were randomly divided into four groups, with each group including ten rats.

**Control group:** No therapy was given to the rats (five rats received saline and five rats received corn oil).

**Ell group:** For ten days, rats were given ellagic acid (10 mg/kg/day).

**Cis group:** Rats were given a single Intraperitoneal (IP) injection of cisplatin (7 mg/kg).

**Cis+Ell group:** Rats were given ellagic acid for 10 days after receiving a single dose of Cis through IP injection.

Cis was given to the animals through IP injection in a single dose of 7 mg/kg (isotonic saline was the vehicle for administering Cis). Ell was dissolved in maize oil at a concentration of 5 mg/ml and administered to animals at a dose of 10 mg/kg/day *via* gavage.

### **Sample collection**

After ten days, the rats were ether anesthetized and killed. The liver and kidney samples were removed and stored away from the light. The liver samples were washed three times in cold isotonic saline (0.9% v/w) and stored at (-20°C) until they were analyzed.

Blood was collected in test tubes from this dislocation and centrifuged to remove serum, before being stored in an Eppendorf tube in a deep freezer at -20°C.

### **Tissue homogenate**

Wash tissue slices in 0.01M PBS before adding the tissue protein extraction reagent in a proportion of 1G: 5-10 ml and mixing in icy water. After blending, centrifuge

the mixture at 5000–10000 rpm for 10 minutes. Take the supernatant immediately after testing or store it at -20°C (for 1–3 months) or -80°C (for 1-3 months).

## **Biochemical Analysis**

### **Estimation of liver function (liver function tests)**

**Determination of ALT and AST:** Kinetic method was used according to the International Federation of Clinical Chemistry by using a Spectrum kit [14].

**Determination of total bilirubin, albumin, and ALP:** Total bilirubin was determined using a Diamond kit [15].

**Determination of total protein:** Total protein was determined by the Biuret method [16].

**Estimation of kidney function (kidney function tests):** Urea, creatinine, and BUN were determined colorimetrically by using a Diamond kit [17].

### **Estimation of antioxidants and MDA**

**Determination of GSH (Glutathione):** Rat glutathione was determined using an ELISA kit [18].

**Determination of SOD (Superoxide Dismutase):** Rat superoxide dismutase was determined using ELISA kit [19].

**Determination of CAT (Catalase):** Rat superoxide catalase was determined using ELISA kit [20].

**Determination of MDA (Malondialdehyde):** Rat Malondialdehyde (MDA) was determined using ELISA kit [21].

### **Estimation of neurotransmitter**

**Determination of glutamate:** Glutamate was determined using ELISA kit [22].

**Determination of Gamma-Aminobutyric Acid (GABA):** Rat GABA was determined using ELISA kit [23].

### **Light microscopy studies**

Specimens from the liver and kidney were fixed in 10% formalin, then dehydrated in increasing degrees of alcohol (70%, 80%, 90%, 95%, and 100%), cleaned in xylene, and embedded in paraffin wax blocks. For the basic histological study, serial slices of 4–6 m thickness were stained with hematoxylin and eosin and Periodic Acid Schiff (PAS) stain to indicate the glycogen content and basement membranes, and Massons trichrome [24] to detect collagen fibers.

### **Immunohistochemical staining**

On paraffin sections (5 m thickness), deparaffinization in xylene, rehydration in descending concentrations of ethanol, and washing in Phosphate Buffer Solution were performed (PBS). To inactivate endogenous peroxidase, 3% hydrogen peroxide was used. The slides were then heated in a citrate buffer (pH 6.0) for 30 minutes at 95°C

to extract antigens. To prevent nonspecific binding, 5% bovine serum albumin in Tris-buffered saline was added. Primary antibodies to P53 (rabbit polyclonal antibody: ab131442) and Bcl2 (rabbit polyclonal antibody: ab196495) were used on liver slides, while anti-COX2 (rabbit monoclonal antibody, ab169782) and anti-caspase 3 (rabbit monoclonal antibody, ab184787) were used on kidney slides. The slides were treated with antibodies at a 1:100 dilution for 60 minutes at room temperature before being rinsed with PBS. To obtain negative control samples, the primary antibodies were eliminated, and slices were counterstained with Mayer's hematoxylin and mounted and viewed under a light microscope. Positive reactions Bcl2 and COX2 showed up as brownish nuclear staining. Caspase 3 was expressed in both the nucleus and cytoplasm [25].

### **Morphometric study and the statistical analysis**

The area percentage of collagen, P53 cell index (number of positive nuclei/total number of nuclei in the same fields  $\times 100$ ), and area percentage of Bcl2 expression in the liver were measured in five nonoverlapping fields from five rats in each group photographed at magnifications of  $10 \times$  (Bcl2) and  $40 \times$  (Bcl2).

In addition to the proximal and distal convoluted tubules' Feret diameter and surface area,  $400\times$  photos were used to calculate glomerular Feret (caliber) diameter, glomerular perimeter, glomerular surface area, and Bowman's (urinary) space for kidney morphometry (Proximal Convoluted Tubules (PCT) and DCT). Measurements were taken in 20 randomly selected glomeruli and 40 tubules in each group of five rats in each group.

Morphometry was performed using ImageJ (FIJI) software. Images were captured using a Leica ICC50W light electric microscope at the Image Analysis Unit of the Anatomy and Embryology Department, Faculty of Medicine, Zagazig University.

### **Statistical analysis**

The information was presented as a mean  $\pm$  standard deviation. To find differences between groups, a one-way Analysis of Variance (ANOVA) was used, followed by Tukey's multiple-comparison post-hoc test. The data were statistically analyzed using GraphPad Prism version 8.0.2 (GraphPad Software, Inc., San Diego, CA). The difference was considered significant when the P-value was less than 0.05.

### **Results**

When compared to the control group, the Cis-treated group had statistically significantly higher mean serum ALT, AST and ALP and had significantly lower mean serum albumin, and total protein levels ( $P < 0.05$ ). When compared to the Cis groups, the Cis+Ell group had significantly lower levels of ALT, AST, and ALP. Moreover, a statistically significant increase of albumin and TP was evident in

the Ell+Cis group compared to Cis groups ( $P < 0.05$ ). The statistical results of the various groups studied are presented in Table 1.

When compared to the control group, the Cis-treated group had statistically significantly higher mean serum urea, creatinine, and BUN levels ( $P < 0.05$ ). When compared to the control group, the Cis group showed significantly higher levels. Moreover, the Ell+Cis group had a statistically significant decrease in serum urea, creatinine, and BUN compared to the Cis group ( $P < 0.05$ ). The statistical results of the groups studied are presented in Table 2.

When compared to the control group, the Cis-treated group had a statistically significant lower mean of GSH, CAT, and SOD ( $P < 0.05$ ), whereas MDA had a significantly higher mean for the same groups. When compared to the control group, the Ell+Cis group had significantly lower levels. Moreover, the Ell+Cis group had a statistically significant increase in GSH, CAT, and SOD compared to the Cis group ( $P < 0.05$ ) but MDA explained a significant decrease in the Ell+Cis group in comparison to the Cis group. The statistical results of the various studied groups are presented in Table 3 (Figure 1).

### **Histopathological Results**

#### **Light microscopic**

**Hematoxylin and eosin:** The histomorphology of the liver and renal cortex in the control and Ell groups was normally (Figures 2a-2c), but the cisplatin group's hepatic tissue was significantly injured (Figures 2d-2f). Hepatocytes with small dark nuclei, thick capsules, a lack of lobular architecture, localised hepatic necrosis, and inflammatory cell infiltrate were all observed. The portal vein branches, the central vein, and the hepatic sinusoids were also dilated and congested. Due to the expansion of bile ducts, the portal area was also extended. Rarely, granuloma with big cells was observed (Figures 2g-2k). Furthermore, the majority of the cisplatin-treated cortical tubules were dilated and necrotic, with casts in the lumina of certain tubules. The periglomerular region was also enlarged, and the renal corpuscles had twisted forms and appeared smaller. The parietal epithelium and macular cells, as well as vacuolate podocytes, showed signs of degeneration. In the interstitium and lumen of DCT, a limited number of inflammatory cells were also discovered. On the other hand, animals administered cisplatin plus ellagic acid at the same time exhibited less hepatic and renal damage. The liver's histoarchitecture was unaltered, the hepatic vasculature was slightly dilated, and apoptotic cells were identified relatively infrequently (Figures 2l-2n). In the kidney, the majority of the glomeruli were also returned to their former size and shape. The tubules in the majority of the animals were similar to those in the control group, and Bowman's capsule was constricted. Despite this, only a few tubules were found to be damaged and dilated (Figure 3).

**Table 1.** Liver function parameters in various studied groups.

	Control	EII	Cis	EII+Cis
ALT (U/L)	29.80 ± 4.89	29.98 ± 5.24	61.69± 7.33 <sup>a</sup>	45.80± 4.14 <sup>a,b</sup>
AST (U/L)	149.4 ± 11.14	142.6 ± 9.46	240.3 ± 19.95 <sup>a</sup>	212.1 ± 8.239 <sup>a,b</sup>
ALP (U/L)	24.64 ± 2.27	22.97 ± 2.14	48.35 ± 2.646 <sup>a</sup>	37.97 ± 2.55 <sup>a,b</sup>
Albumin (g/dl)	3.988 ± 0.1385	4.041 ± 0.1445	3.183 ± 0.2129 <sup>a</sup>	3.326 ± 0.2486 <sup>a,b</sup>
Total protein (TP) (g/dl)	7.627 ± 0.256	7.856 ± 0.262	5.453 ± 0.416 <sup>a</sup>	6.451 ± 0.557 <sup>a,b</sup>
Total bilirubin (mg/dl)	0.5700 ± 0.03830	0.5270 ± 0.04218	2.858 ± 0.3219 <sup>a</sup>	1.826 ± 0.5427 <sup>a,b</sup>

**Note:** All values are expressed as mean ± SD, n=10. <sup>a</sup>Significant vs. control group. <sup>b</sup>Significant vs. Cis.

**Table 2.** Serum creatinine, urea, BUN, and total bilirubin in various studied groups.

Parameter	Control	EII	Cis	EII+Cis
Creatinine (mg/dl)	0.3690 ± 0.07564	0.3480 ± 0.06779	1.343 ± 0.4408 <sup>a</sup>	0.7230 ± 0.03683 <sup>a,b</sup>
Urea (mg/dl)	31.82 ± 4.139	29.32 ± 4.739	69.00 ± 12.28 <sup>a</sup>	44.48 ± 4.214 <sup>a,b</sup>
BUN (mg/dl)	14.85 ± 1.919	14.19 ± 2.316	32.64 ± 3.946 <sup>a</sup>	20.12 ± 2.009 <sup>a,b</sup>

**Note:** All values are expressed as mean ± SD, n=10. <sup>a</sup>Significant vs. control group. <sup>b</sup>Significant vs. Cis.

**Table 3.** Tissue homogenate antioxidant enzyme levels and MDA in various studied groups.

Parameter	Control	EII	Cis	EII+Cis
GSH (ng/mg)	191.8 ± 12.66	193.1 ± 11.92	31.20 ± 5.673 <sup>a</sup>	74.35 ± 8.152 <sup>a,b</sup>
CAT (ng/mg)	10.09 ± 0.7418	10.26 ± 0.6949	0.6110 ± 0.09585 <sup>a</sup>	3.435 ± 1.384 <sup>a,b</sup>
SOD (U/mg)	203.5 ± 20.30	205.1 ± 19.53	39.58 ± 5.994 <sup>a</sup>	93.16 ± 5.214 <sup>a,b</sup>
MDA (nmol/mg)	3.340 ± 0.6970	2.937 ± 0.8360	30.40 ± 4.492 <sup>a</sup>	20.28 ± 2.320 <sup>a,b</sup>

**Note:** All values are expressed as mean ± SD, n=10. <sup>a</sup>Significant vs. control group. <sup>b</sup>Significant vs. Cis.

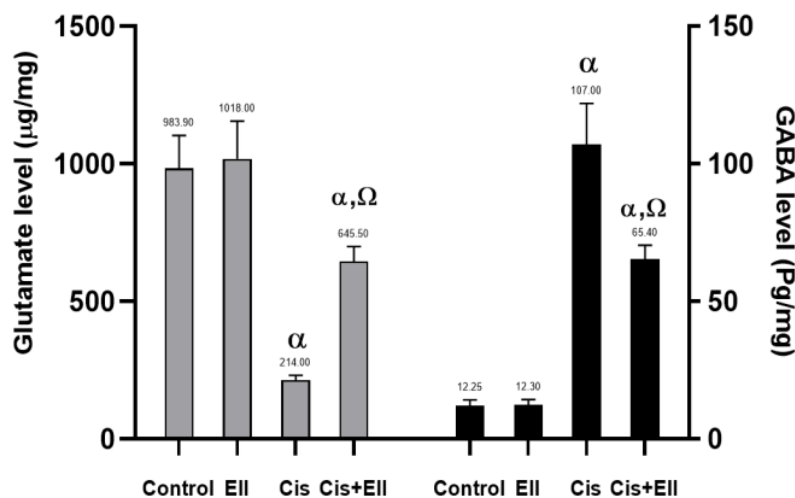


**Figure 1.** Glutamate and GABA levels were measured in various study groups. One-way ANOVA was used for statistical analysis, followed by Tukey's post-hoc test. The values are shown as mean ± SE (n=10). α-significant difference from the control group P<0.05 and Ω-significant difference from the Cis group P<0.05. Note: (■) Glutamate, (▒) GABA

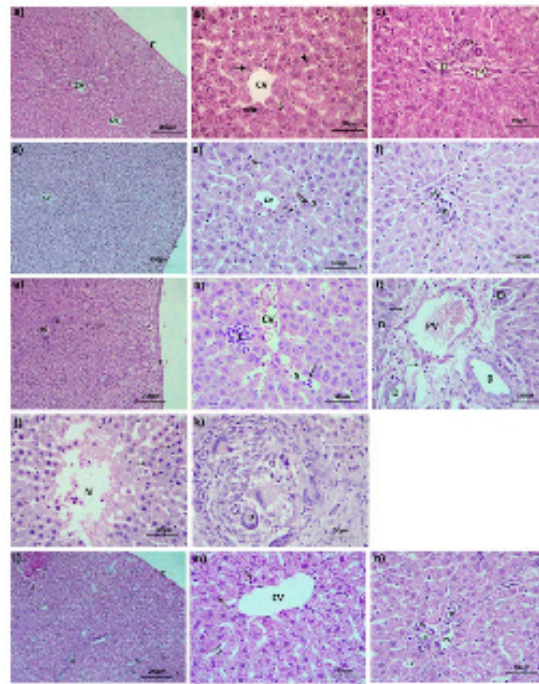


**Figure 2.** H and E-stained adult rat liver sections from the control group (a-c) and the Ell group (d-f) show parts of hepatic lobules with normal histoarchitecture and thin capsule (c); cords of Hepatocytes (H) branching from the Central Vein (CV) separated by narrow sinusoids (S) with few Kupffer cells (arrowhead) inside; liver cells appear polyhedral with eosinophil cytoplasm. (g-k) demonstrates g: thickened capsule (C) with hepatic architecture loss. h: cellular infiltrate (I), dilated congested CV, dilated congested hepatic sinusoid (s) with inflammatory cells inside (arrow); i: portal area with extensive CT (arrows), dilated congested portal vein, and proliferation and hyperplasia of bile ducts; j) hepatic tissue necrosis and hepatocytes with pyknotic nuclei; and k) granuloma with giant cell (G) (a, d, g, and l: H and E,  $\times 100$ ; b, c, e, f, h, i, j, k, m, and n: H and E,  $\times 400$ ).

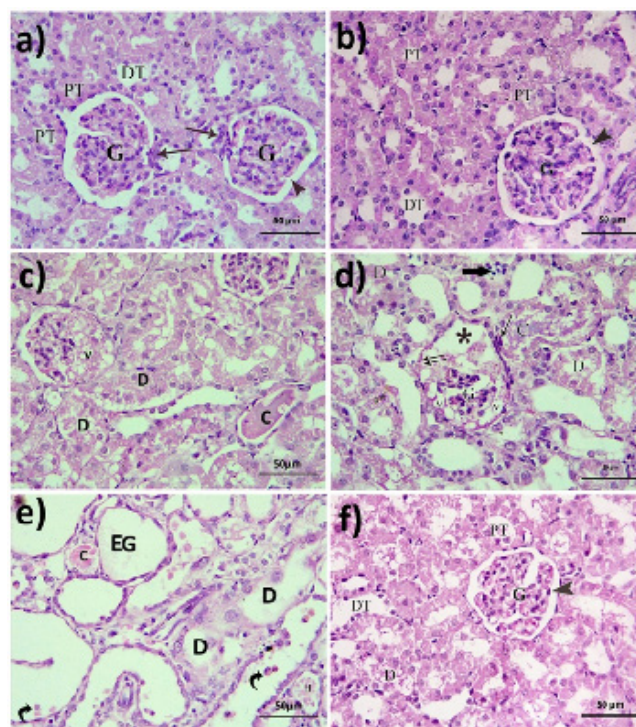


**Figure 3.** Photomicrographs of histological sections of adult rats' renal cortex. Normal histological appearance of the cortex in the control (a) and Ell (b) groups: rounded regular glomeruli (G) bordered by narrow Bowman's gap (arrowhead). There is evidence of the macula densa (arrow), Proximal convoluted Tubules (PT), and Distal convoluted Tubules (DT). The cisplatin group (c-e) had enhanced tubular necrosis (D), tubular casts (C), intratubular hemorrhage (H), dilated tubules with white (curved arrow) within, and interstitial inflammatory cells in the cortex of the kidney (thick arrow). The glomeruli were also smaller and irregular, with a dilated urinary gap (star), podocyte vacuolization, and degeneration of parietal (double arrow) and macular cells (arrow). Occasionally, empty glomeruli were seen. The Cis+Ell rats' kidney (f) has a largely normal glomerulus (G) with a narrow urine space (arrowhead), PT, few dilated DT, and few degraded tubules (D). (H and E,  $\times 400$ ).

**Periodic acid Schiff:** In rats given either vehicle or Ell in the liver, PAS-positive inclusions filled the cytoplasm of the majority of hepatocytes (Figures 4a and 4b). Although the liver cells of rats given only Cis were negative for PAS, a thicker basement membrane of the principal vein demonstrated a strong positive response (Figure 4c). In rats given both Ell and Cis, a positive response was seen in certain hepatocytes as well as the relatively thin endothelial basement membrane (Figure 4d). Both the control group (Figure 5a) and Ell-treated (Figure 5b) groups of rats had thin PAS-stained basement membranes encircling both tubules and glomeruli, as well as a thick PAS-positive brush border of the PCT in the renal cortex stained with PAS. In contrast, Cis-treated rats had thickened glomerular and tubular basement membranes with a thin interrupted brush border (Figure 5c). The Cis+Ell group had a narrow Bowman's capsule and a continuous brush boundary (Figure 5d).

**Masson's trichrome:** The control and Ell groups had an average collagen distribution in both the kidneys (Figures 6a-6d) and the liver (Figures 7a and 7b). In the Cis-treated rats, there was excessive collagen fiber deposition in the portal area and the wall of hepatic sinusoids, as well as the glomerulus and the wall of renal blood vessels (Figure 7c). Rats given both Ell and Cis had less collagen in their hepatic and renal tissues (Figure 7d).

#### **Immunohistochemical results**

**Immunohistochemistry of P53:** Anti-P53 antibodies

were not detected in the hepatocytes of rats given either vehicle or Ell. The nuclei of liver cells near the hepatic lobule periphery, on the other hand, were significantly stained with anti-P53 antibodies. Only a few hepatocytes were immunoreactive in rats given Ell and Cis (Figure 8).

**Immunoreaction of Bcl2:** In both control and Ell-treated animals, Bcl2 was found in high concentration in the cytoplasm of liver cells. In the Cis group of rats, immunoreaction was negative. Immunoreactivity was found in the rat hepatocytes of the Cis+Ell group (Figure 9).

**Anti-COX2 immunostaining:** In anti-COX2 immunostained kidney sections, both the control and Ell groups showed negative immunoreactivity. Cis elicited a strong cytoplasmic response in the epithelial cells of the cortical tubules and parietal cells of renal corpuscles. Rats were treated with Cis and Ell. Some tubular epithelial cells showed a minor reactivity (Figure 10).

**Expression of caspase 3:** When stained with anti-caspase 3, the rats in the control and Ell groups showed weak immunoreactivity in their renal tissue. However, in the Cis group, there was a strong positive reaction in the nuclei of tubular, parietal, and mesangial cells, and in the Cis+ellagic group, there was only a weak positive reaction in certain tubular cells (Figure 11).

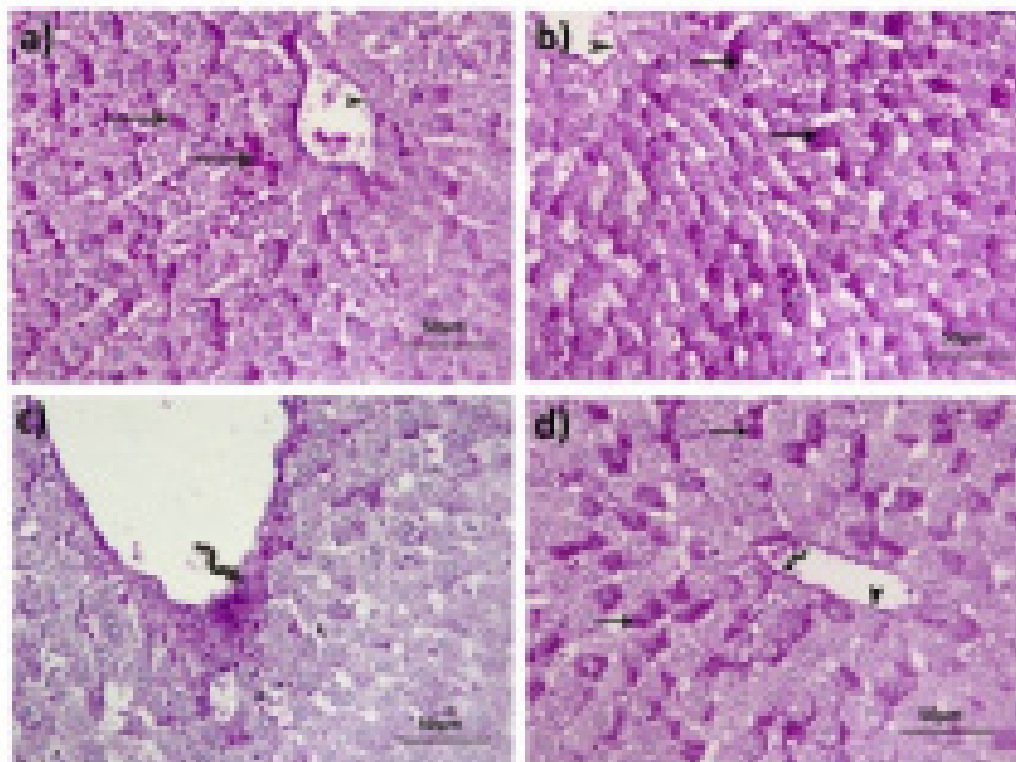


**Figure 4.** Strong PAS-positive cytoplasmic inclusions (arrows) in the liver cells and thin basement membrane of the central vein (arrowhead) in both control (a) and ellagic acid (b) groups; negative PAS reaction in the hepatocytes and accentuated PAS staining around the central vein (wavy arrow) in the cisplatin group (c); and magenta staining of the cytoplasm of hepatocytic cytoplasm and basement membrane (d) (PAS × 400).

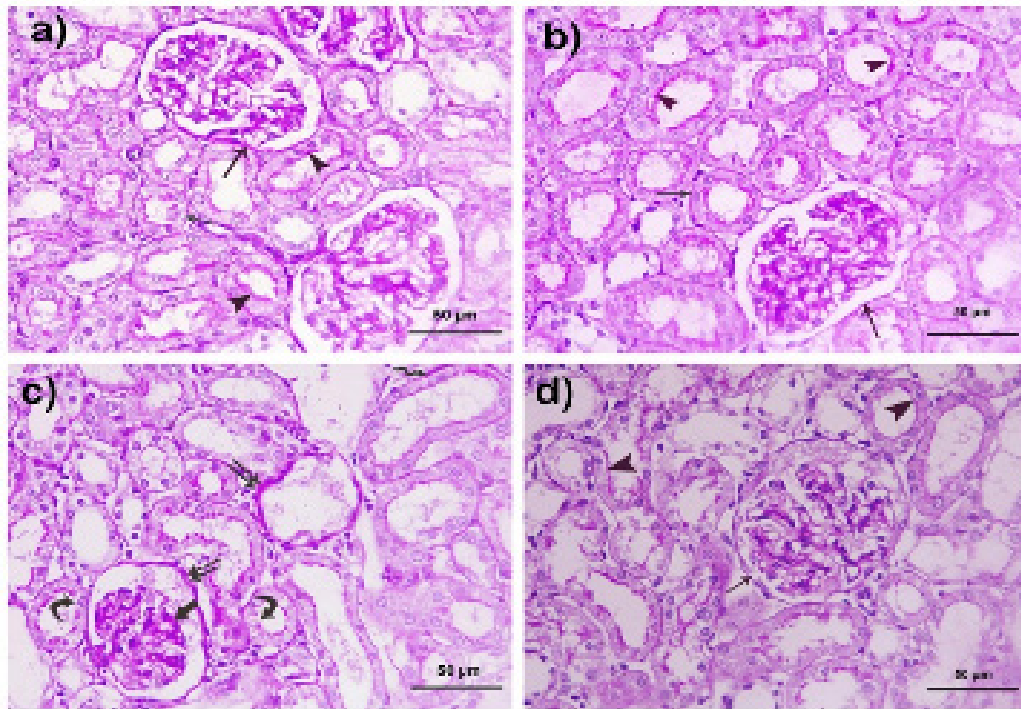


**Figure 5.** PAS-stained slices of an adult rat's renal cortex photographed under a microscope. Bowman's capsule and tubular basement membranes (arrow) show thin positive staining in the ellagic acid (a) and control (b) groups, as well as a positive thick reaction in the tubular brush border (arrowhead). In the cisplatin group (c), the basement membranes of Bowman's capsule (double arrow), glomerulus (thick arrow), and tubules (wavy arrow) thicken, and the brush border of tubular epithelium is lost (curved arrow). A thin foundation membrane (arrow) and a continuous brush boundary (arrowhead) may be seen in rats given cisplatin and ellagic acid (d) (PAS,  $\times 400$ ).

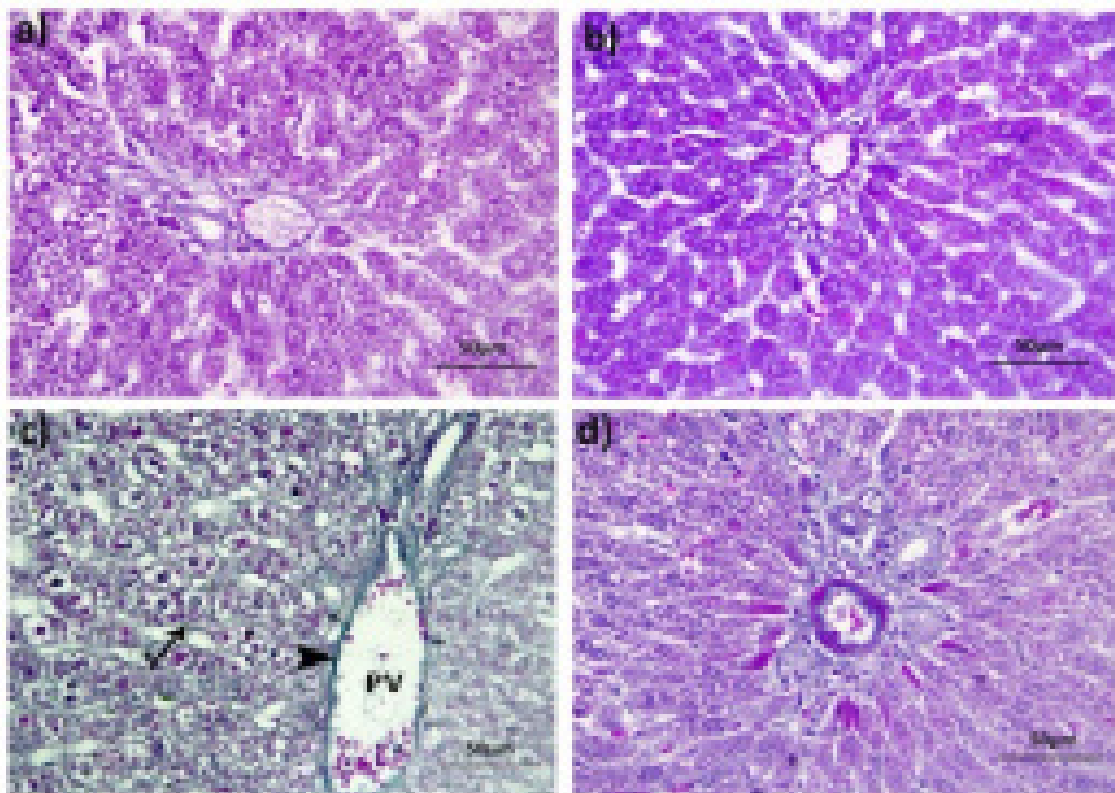


**Figure 6.** In both the control a) and ellagic b) groups, adult rat liver sections stained with Masson's trichrome show normal collagen fiber distribution in the portal region and sinusoidal wall. Collagen fibers deposition (arrowhead) around the portal vein and in the sinusoidal wall is greater in the cisplatin group c) (arrow). There is an obvious decrease in collagen around the structures in the portal area in the cisplatin+ellagic group (d) (a-d:  $\times 400$ ).

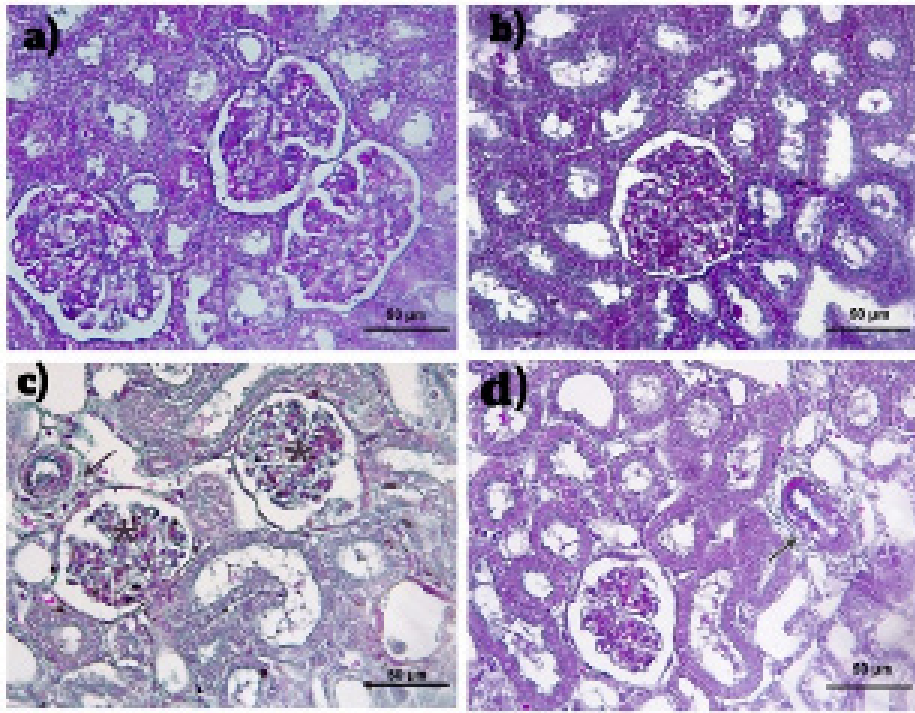


**Figure 7.** Adult rats' renal cortex photomicrographed with Masson's trichrome-stained slices. In both the control (a) and ellagic (b) groups, collagen fibers around renal corpuscles are thin. In the cisplatin group, there are dense, green-stained collagen fibers around blood vessels (arrow) and in the mesangial matrix in the cisplatin group (c) (asterisks). The Cis+Ell group (d) (arrow) had less collagen deposition (Masson,  $\times 400$ ).

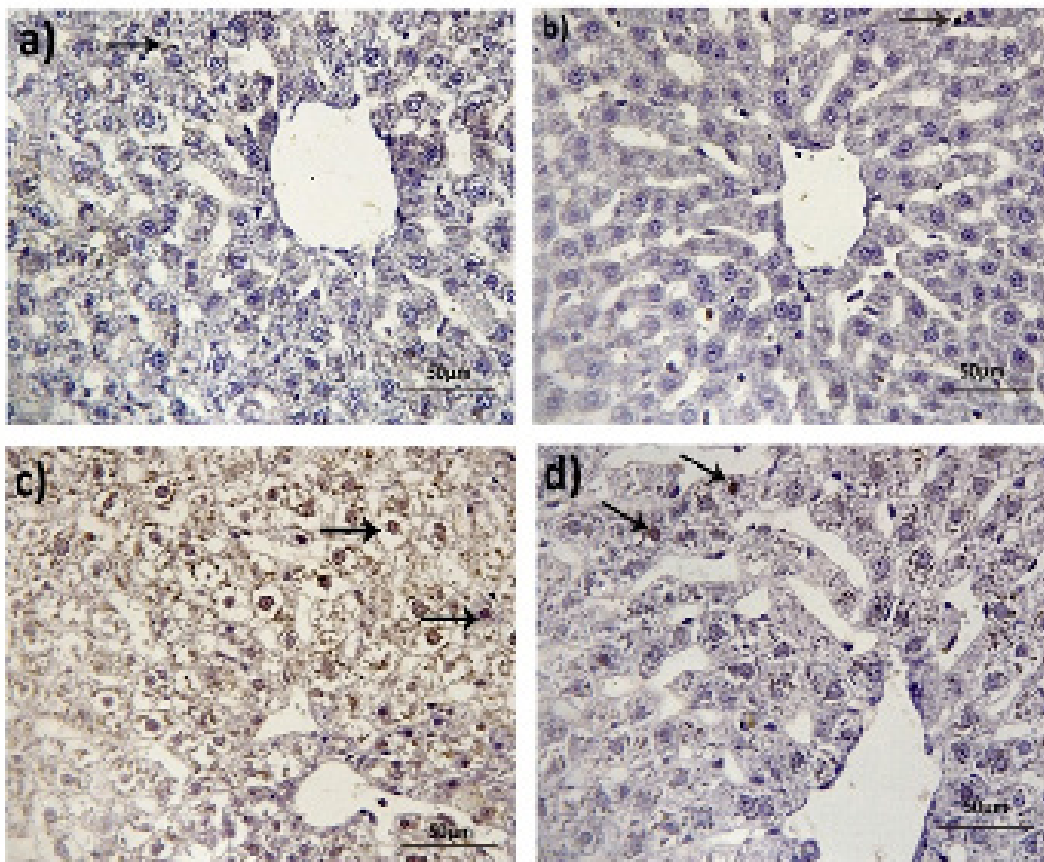


**Figure 8.** P53 staining of adult rat liver sections reveals a negative reactivity in both the control a) and ellagic b) groups. Cisplatin group c), on the other hand, causes a strong nuclear reaction in hepatic cells, particularly at the lobule's periphery (arrow). In the cisplatin+ellagic group, there are few hepatocytes with immunostaining in their nuclei d) (a-d: anti-P53  $\times 400$ ).

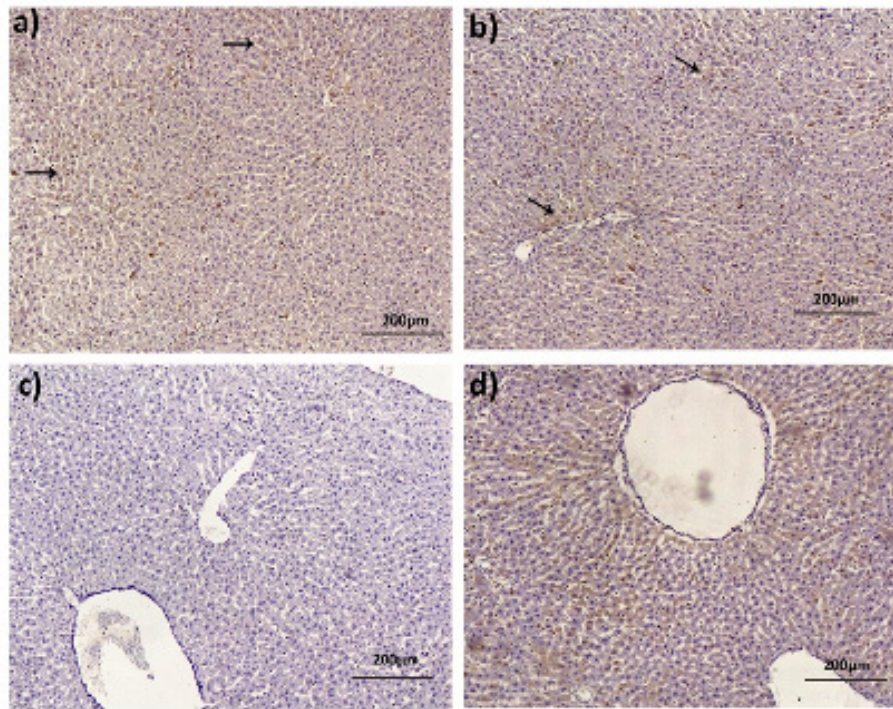


**Figure 9.** Positive immunoreaction (arrows) in the cytoplasm of liver cells in both the control a) and ellagic b) groups; negative reaction in the cisplatin c) group. Adult rat liver sections immunostained for Bcl2 show positive immunoreactions (arrows) in the cytoplasm of liver cells in both the control a) and ellagic b) groups, but a negative reaction in the cisplatin group c). Immunoreactivity is stored in the cisplatin+ellagic group (a-d:  $\times 400$ ).

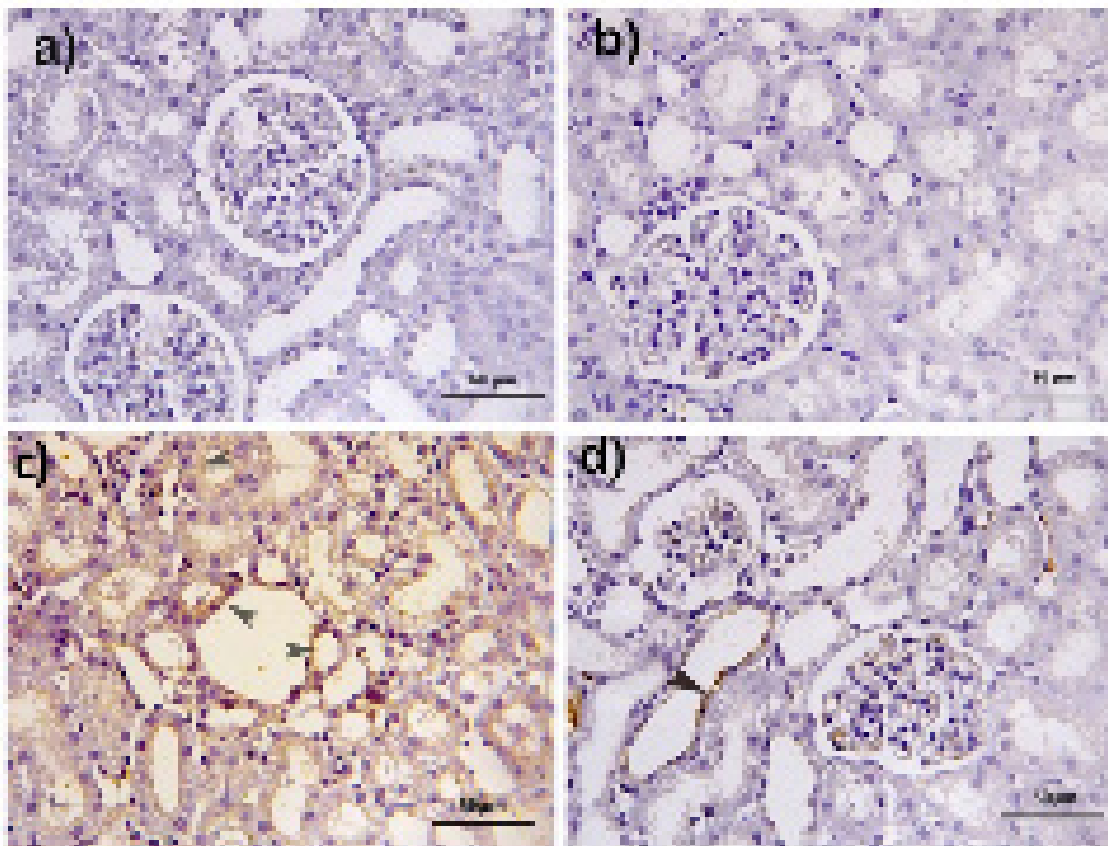


**Figure 10.** Anti-COX2 immunostained slices of adult rats' renal cortex are shown in photomicrographs. In both the control (a) and ellagic (b) groups, the anti-COX2 reaction in renal corpuscles and the tubular epithelium is negative. There is a high cytoplasmic immunoreaction (arrowheads) in cells lining tubules and glomerular parietal cells in the cisplatin group (c) Cisplatin and ellagic acid-treated rats (d) had moderate immunostaining in the epithelial cells of certain tubules (arrowhead) (anti-COX2,  $\times 400$ ).

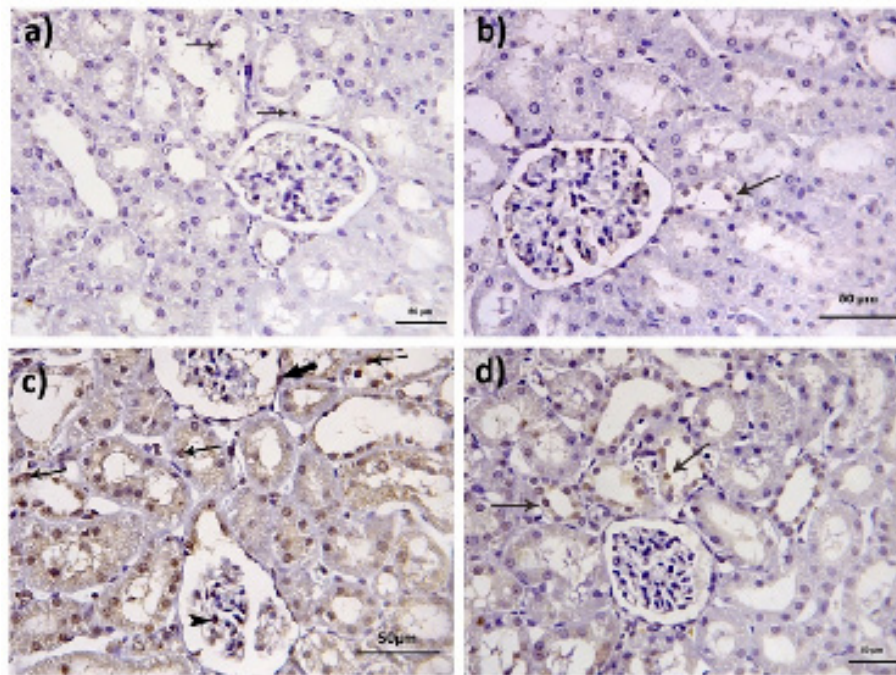


**Figure 11.** Caspases 3 immunostained slices in of adult rat renal cortex of adult rats photomicrographed. Few cells in the control (a) and ellagic (b) groups exhibit modest nuclear expression (arrow). In the cisplatin group (c) mesangial cells (arrowhead), parietal cells (thick arrow), and tubule lining show a strong nuclear immunoreaction (arrows). Some tubular epithelial cells in rats treated with cisplatin plus ellagic acid (d) (arrows) show moderate reactivity (Anti-caspase 3,  $\times 400$ ).

## Discussion

Experimental drug-induced hepatorenal toxicity can be used to study the complex biology of drug harm. Rodents provide a basic model that is similar to Cis-induced nephrotoxicity in humans [26,27] and can be used to assess potential protective medicines. Cis was given through IP injection because this is the most common way of giving Cis to rodents [28].

According to current evidence, Cis can impair liver function by increasing levels of liver function biomarkers such as ALT and AST. These findings appear to corroborate those of Palipoch and Punsawad [29]. They discovered that Cis treatment has a harmful effect on the liver. Serum aminotransferases (ALT and AST) are hepatocyte cytosolic enzymes; an increase in their activity reflects an increase in hepatocyte plasma membrane permeability, which is linked to cell death [30]. Cis also causes mitochondrial dysfunction, especially the inhibition of the electron transport system, which leads to an increase in the production of superoxide anions,  $H_2O_2$ , and hydroxyl radicals [31].

According to our histological findings, biliary radicals grew in the liver specimens of Cis-treated mice. Because of the unfavorable effect of Cis, a significant increase in ALP activity may indicate liver abnormalities and cholestasis. As a result of biliary obstructions or cholestasis, the ALP activity rises, making it a biomarker for hepatobiliary illness [32]. Furthermore, a change in serum bilirubin levels is a biochemical signal of changes in the morphological integrity of the hepatobiliary tract,

which is a marker of liver injury [33]. Cis toxicity resulted in a significant decrease in serum total protein, albumin, and globulin levels [34].

The primary Cis hepatotoxicity is the increase in free radical formation, a decrease in antioxidant system effectiveness, and an increase in apoptotic pathways. Despite this, no one has a complete understanding of the underlying pathophysiology [35]. Routine histological liver slices from the Cis group in this investigation indicated a loss of lobular organization, localized necrosis, apoptosis of hepatocytes, dilated congested hepatic vasculature, and inflammation, in agreement with the results of Elkomy *et al.*, [36]. Cis reduced hepatocyte glycogen reserves, as demonstrated by a negative PAS reaction [37]. The appearance of inflammatory granulomas with large cells in Cis-intoxicated rats' hepatic lobules was an exciting result. According to Rzczycki *et al.*, [38], granulomatous inflammation could be one of the drug-induced liver injuries.

In this study, Cis also increased fibrous tissue in the hepatic lobule. Tumor Growth Factor-1 (TGF-1) expression is frequently elevated in Cis-induced hepatic fibrosis [39]. Cis, according to Xu *et al.*, [40], can prevent postoperative laryngeal stenosis in human vocal fold fibroblasts by inducing antiproliferative and antifibrotic changes.

The tumor protein p53 interacts with members of the Bcl2 proteins family in a transcription-independent manner, which is required for Cis-induced apoptosis. A study reported that Cis induced an intense nuclear immune expression of P53 in rat hepatocytes while simultaneous

downregulation of Bcl2 expression, similar to the current study.

In large investigations, natural products have been proven to decrease Cis-induced hepatotoxicity. Ell is thought to have anti-inflammatory and antiapoptotic properties in magnocellular systems. Furthermore, in mice, Ell-enhanced hepatic redox status controlled proinflammatory cytokine levels and reduced the histopathology of alcohol-induced liver disease. In this study, Ell altered the hepatic histoarchitecture, regenerated hepatocyte glycogen stores, and significantly reduced collagen deposition in the liver in the Cis+Ell group. Besides inactivating hepatic stellate cells, Ell has antifibrotic molecular mechanisms that include inhibiting proteins that promote fibrogenesis.

According to the current findings, Ell induced a significant recovery in all biochemical activities of the liver, where Ell has demonstrated scavenging capacity against a variety of ROS. Ell protects hepatocytes from Cis-induced damage by acting as a ROS scavenger and maintaining antioxidant enzyme levels [8]. However, it is unknown whether Ell effects are mediated by Nrf2 activation and/or whether this antioxidant affects mitochondrial dysfunction, which has been linked to Cis-induced hepatotoxicity [9].

The antiapoptotic properties of Ell were demonstrated by a significant decrease in the P53 positive cell index and an increase in the expression of the antiapoptotic protein Bcl2. The hepatoprotective activity of *Ganoderma lucidum* against Cis-induced hepatotoxicity was mediated by a decrease in P53 expression and an increase in the Bcl2 expression. Furthermore, Ell reduced cyclophosphamide-induced P53 immunoreactivity in rat liver and heart. Nonetheless, p53 activation has been shown to promote survival in acetaminophen-induced hepatotoxicity. When stress is mild, P53 pauses the cell cycle, encouraging DNA repair and cell survival; however, when DNA is significantly damaged, P53 activates the promotion of apoptotic genes and downregulates Bcl2, resulting in cell death.

Significant nephrotoxicity was observed following Cis treatment, as evidenced by an increase in serum creatinine, urea, and BUN levels. Several processes were used to explain these effects including the formation of reactive oxygen and nitrogen species, inflammation, and apoptosis. The former disrupts the antioxidant defense system, causing oxidative damage to tissues as well as a reaction with thiols in proteins and glutathione, resulting in cell malfunction. Damage to the renal epithelial cells may trigger inflammation, which can aggravate renal injury and dysfunction *in vivo*.

Cis has a cumulative and dose-dependent nephrotoxic effect. Acute kidney injury following a single Cis injection is thought to be caused by proximal tubular cell necrosis and apoptosis caused by an impaired antioxidant system, inflammatory responses, and vascular injury. Because Cis is a small molecule, it can easily pass through the

glomerular basement membrane and reach the PCT. In tubular epithelial cells, Cis is converted to a highly reactive Cis-thiol compound.

According to the histological and morphometrical analysis of H&E-stained kidney slides, the destructive effects of Cis on renal tubules and corpuscles were similar to the previous literature. Bowman's capsule enlargement and shrinking glomeruli were observed in rats given Cis 7 mg/kg, 7.5 mg/kg, and 16 mg/kg. According to Dupre *et al.*, Cis stimulates fibrogenic cells in the kidney by increasing the activity of hedgehogs and other signaling pathways. TGF-1 is acquired by tubular epithelial cells to differentiate into matrix-producing myofibroblasts. In the Cis group, collagen deposition was visible in the mesangium and interstitium of renal tissue stained with Masson's trichrome.

Cis-induced apoptosis of tubular and mesangial cells was linked to increased levels of COX2 mRNA and protein levels. The activation of the COX2/PGE2 pathway causes inflammatory renal disease. Caspases, particularly caspase 3, are also the primary mechanism of programmed cell death. In cultured mouse proximal tubular epithelial cells, Cis promoted dosage and time-dependent caspase 3 cleavage. In this study, Cis therapy increased COX2 and caspase 3 expressions in the renal tissue of the Cis group compared to the control group.

There is an urgent need for clinical trials of a safe and effective renoprotective drug as an adjunct therapy for patients receiving high doses of Cis. According to our findings, Ell can correct urea, creatinine, and BUN concentrations, with Ell's antioxidant mechanism being the activation of cellular antioxidant systems or direct activity as an antioxidant factor. This polyphenol is sometimes used as an antioxidant supplement during Cis chemotherapy and protects against cancer. Furthermore, after Ell treatment of a Cis-intoxicated kidney, the glomeruli's recovery to normal, inflammatory cells was not observed, and tubular necrosis was limited to a few tubules. Furthermore, morphometric measurements of the glomerular and distal tubules were used as controls, with significant improvements in PCT diameter and surface area.

A study by Li *et al.*, found that Ell reduced bleomycin-induced lung fibrosis in mice by inhibiting myofibroblast activation and increasing myofibroblast autophagy and death. In this study, the antifibrotic action of Ell was validated by improvements in the Cis+Ell group's histological and morphological data of the kidney when compared to the Cis group.

The pharmacological inhibition of COX enzyme activity is an effective treatment for several medical conditions. Limiting COX2 was shown to significantly reduce Cis-induced mesangial cell apoptosis. The amelioration of gentamicin-induced renal injury and diabetic nephropathy was linked to a decrease in caspase 3 protein levels and an

increase in Bcl2 protein levels in the kidney of rats given 10 mg/kg Ell. Similarly, Ell reduced COX2 and caspase 3 immunoreactivity in the cortices of rats given Cis and Ell.

Our brain homogenate study after Cis treatment revealed a significant increase in glutamate levels and a significant decrease in GABA in rat brains. These findings support the findings of Abdelkader *et al.*, who discovered that Cis administration was linked to a decrease in GABA and an increase in glutamate levels in the hippocampi and cortex of rats, implying that Cis use is linked to depression. This psychological dysfunction is caused either directly by nephrotoxicity or indirectly by changes in neurotransmitter levels as well as histopathological abnormalities. There is a clear link in the brain between cognitive impairment and GABA levels. Cis increased the glutamate content of the rat hippocampus and cortex.

When Ell was administered, the Cis-induced decrement in brain GABA levels and glutamate increase were significantly reversed. These findings are consistent with those of Dhingra and Jangra, who discovered that Ell had a significant antiepileptic effect in mice, probably due to an increase in GABA levels in the brain.

## Conclusion

According to the study, the activity of the key scavenger enzymes (SOD, CAT, and GSH) was significantly reduced in the livers of Cis-treated rats. When rats were given Cis, they developed severe kidney failure, as evidenced by a significant increase in blood BUN and uric acid concentrations, as well as increased kidney MDA and decreased GSH, SOD, and CAT activities. The fact that Cis treatment is linked to an increase in free radical production, severe oxidative stress, and lipid peroxidation explains these findings. Cis has previously been shown to cause oxidative damage and lipid peroxidation in kidney tissues in previous studies. The amount of MDA, an important measure of oxidative stress, increased in Cis-intoxicated rats, resulting in glutathione and other endogenous antioxidants such as SOD and CAT. Ell treatment reversed the Cis results by protecting against lipid peroxidation and the formation of free radical derivatives, as evidenced by lower levels of lipid peroxidation markers. Ell protects cells from lipid peroxidation and thus oxidative stress by scavenging free radicals.

To summarize, Ell effectively mitigated Cis-induced hepato-, nephron-, and neurotoxicity by restoring all biomarkers in the liver, kidney, and brain homogenates, as well as histomorphological alterations in rat hepatic and kidney tissues, by modulating the COX2/caspase 3 and P53/Bcl2 pathways.

## Acknowledgement

I am grateful to those who instilled in me the value of education and the rewards and opportunities it can generate for my parents, especially my father, who supplied me

with enthusiasm, support, and creative insight. His critical reading of the manuscript helped me refine the concept of this thesis; his deep interest in the topic, and unflinching encouragement are highly appreciated.

## Author's Contribution

HA, AD, and AG conceived and designed the research. HA and NG conducted experiments and biochemical analysis. HA and JA contributed new analytical tools and histopathological studies. HA and JA analyzed the data. HA, NG and JA wrote the manuscript. All authors read and approved the manuscript.

## Ethics Approval and Consent to Participate

All animal procedures were carried out with the approval of the Ethics Committee of the National Research Center, Egypt, and following recommendations of the institutional animal care and use committee of the Zagazig University (ZU-IACUC/3/f/21/2021).

## References

1. Ojima T, Nakamura M, Nakamori M, Katsuda M, Hayata K, Maruoka S. Phase I/II trial of chemotherapy with docetaxel, cisplatin, and S-1 for unresectable advanced squamous cell carcinoma of the esophagus. *Oncology* 2018; 95: 116-120.
2. Lu Y, Cederbaum AI. Cisplatin-induced hepatotoxicity is enhanced by elevated expression of cytochrome P450 2E1. *Toxicol Sci* 2006; 89: 515-523.
3. Attyah AM, Ismail S. Protective Effect of Ginger Extract against Cisplatin-Induced Hepatotoxicity and Cardiotoxicity in Rats. *Iraqi J Pharm Sci* 2012; 21: 27-33. [Google Scholar]
4. Kang DG, Lee AS, Mun YJ, Woo WH, Kim YC, Sohn EJ. Butein ameliorates renal concentrating ability in cisplatin-induced acute renal failure in rats. *Biol Pharm Bull* 2004; 27: 366-370.
5. Devipriya N, Srinivasan M, Sudheer A, Menon VJ. Effect of ellagic acid, a natural polyphenol, on alcohol-induced prooxidant and antioxidant imbalance: A drug dose dependent study. *Singapore Med J* 2007; 48: 311.
6. Kannan MM, Quine SD. Ellagic acid ameliorates isoproterenol induced oxidative stress: Evidence from electrocardiological, biochemical and histological study. *Eur J Pharmacol* 2011; 659: 45-52.
7. Rosillo M, Sanchez-Hidalgo M, Cárdeno A, de La Lastra CA. Protective effect of ellagic acid, a natural polyphenolic compound, in a murine model of Crohn's disease. *Biochem Pharmacol* 2011; 82: 737-745.
8. Yüce A, Ateşşahin A, Çeribaşı AO, Aksakal M. Ellagic acid prevents cisplatin-induced oxidative stress in liver and heart tissue of rats. *Basic Clin Pharmacol Toxicol* 2007; 101: 345-349.
9. Waseem M, Parvez SJ. Mitochondrial dysfunction mediated cisplatin induced toxicity: Modulatory role of curcumin. *Food Chem Toxicol* 2013; 53: 334-342.
10. Hassoun EA, Vodhanel J, Abushaban AJ. The modulatory effects of ellagic acid and vitamin E succinate on TCDD-induced oxidative stress in different brain regions of rats after subchronic exposure. *J Biochem Mol Toxicol* 2004; 18: 196-203.

11. Seeram NP, Adams LS, Henning SM, Niu Y, Zhang Y, Nair MG. *In vitro* antiproliferative, apoptotic and antioxidant activities of punicalagin, ellagic acid and a total pomegranate tannin extract are enhanced in combination with other polyphenols as found in pomegranate juice. *J Nutr Biochem* 2005; 16: 360-367.
12. Iino T, Nakahara K, Miki W, Kiso Y, Ogawa Y, Kato S. Less damaging effect of whisky in rat stomachs in comparison with pure ethanol. *Digestion* 2001; 64: 214-221.
13. Tian L, Shi MM, Forman HJ. Increased transcription of the regulatory subunit of  $\gamma$ -glutamylcysteine synthetase in rat lung epithelial L2 cells exposed to oxidative stress or glutathione depletion. *Arch Biochem Biophys* 1997; 342: 126-133.
14. Breuer J. Report on the symposium" Drug effects in Clinical Chemistry Methods". *Eur J Clin Chem Clin Biochem* 1996; 34: 385-386.
15. Young DS. *Effects of disease on Clinical Lab.* 4th Ed 2001.
16. Cannon D, Olitzky P, Harper NY. *Proteins.* 1974: 422-428.
17. Burtis CA, Ashwood ERJP. *Tietz textbook of clinical chemistry.* 1999; 1654-1655.
18. Jawaid P, Rehman MU, Zhao QL, Misawa M, Ishikawa K, Hori M. Small size gold nanoparticles enhance apoptosis-induced by cold atmospheric plasma *via* depletion of intracellular GSH and modification of oxidative stress. *Cell Death Discovery* 2020; 6: 1-12.
19. Sayed AAR. Ferulic acid modulates SOD, GSH, and antioxidant enzymes in diabetic kidney. *Evid Based Complement Alternat Med* 2012; 580104.
20. Chelikani P, Fita I. Diversity of structures and properties among catalases. *Cell Mol Life Sci* 2004; 61: 192-208.
21. Sohail MU, Al-Mansoori L, Al-Jaber H, Georgakopoulos C, Donati F, Botrè F. Assessment of Serum Cytokines and Oxidative Stress Markers in Elite Athletes Reveals Unique Profiles Associated With Different Sport Disciplines. *Front Physiol* 2020; 11: 1317.
22. Kaneko Y, Pappas C, Malapira T, Vale FL, Tajiri N. Extracellular HMGB1 modulates glutamate metabolism associated with kainic acid-induced epilepsy-like hyperactivity in primary rat neural cells. *Cell Physiol Biochem* 2017; 41: 947-959.
23. Patterson E, Ryan PM, Wiley N, Carafa I, Sherwin E, Moloney G. Gamma-aminobutyric acid-producing lactobacilli positively affect metabolism and depressive-like behaviour in a mouse model of metabolic syndrome. *Sci Rep* 2019; 9: 1-15.
24. Suvarna KS, Layton C, Bancroft JD. *Bancroft's theory and practice of histological techniques.* 8<sup>th</sup> Ed 2018.
25. Kiernan JA. *Histological and histochemical methods: Theory and practice.* *Eur J Histochem* 1999; 12: 479.
26. McGill MR, Jaeschke H. Animal models of drug-induced liver injury. *Biochim Biophys Acta Mol Basis Dis* 2019; 1865: 1031-1039.
27. Holditch SJ, Brown CN, Lombardi AM, Nguyen KN, Edelstein C. Recent advances in models, mechanisms, biomarkers, and interventions in cisplatin-induced acute kidney injury. *Int J Mol Sci* 2019; 20: 3011.
28. Perse M, Veceric-Haler Z. Cisplatin-induced rodent model of kidney injury: Characteristics and challenges. *Biomed Res Int* 2018.
29. Palipoch S, Punsawad CJ. Biochemical and histological study of rat liver and kidney injury induced by cisplatin. *J Toxicol Pathol* 2013; 26: 293-299.
30. Rosen HJ. Laboratory evaluation of the patient with signs and symptoms of liver disease. 1998: 812-820.
31. Chang B, Nishikawa M, Sato E, Utsumi K. L-Carnitine inhibits cisplatin-induced injury of the kidney and small intestine. *Arch Biochem Biophys* 2002; 405: 55-64.
32. El-Hosseiny L, Alqurashy N, Sheweita S. Oxidative stress alleviation by sage essential oil in co-amoxiclav induced hepatotoxicity in rats. *Int J Biomed Sci* 2016; 12: 71.
33. Alqasoumi SI. Evaluation of the hepatoprotective and nephroprotective activities of *Scrophularia hypericifolia* growing in Saudi Arabia. *Saudi Pharm J* 2014; 22: 258-263.
34. Shibayama K, Wachino Ji, Arakawa Y, Saidijam M, Rutherford NG, Henderson PJM. Metabolism of glutamine and glutathione *via*  $\gamma$ -glutamyltranspeptidase and glutamate transport in *Helicobacter pylori*: possible significance in the pathophysiology of the organism. *Mol Microbiol* 2007; 64: 396-406.
35. Man Q, Deng Y, Li P, Ma J, Yang Z, Yang X. Licorice ameliorates cisplatin-induced hepatotoxicity through antiapoptosis, antioxidative stress, anti-inflammation, and acceleration of metabolism. *Front Pharmacol* 2020; 11: 1702.
36. Elkomy A, Abdelhiee EY, Fadl SE, Emam MA, Gad FAM, Sallam A. L-Carnitine mitigates oxidative stress and disorganization of cytoskeleton intermediate filaments in cisplatin-induced hepato-renal toxicity in rats. *Front Pharmacol* 2020: 1548.
37. Bilgic Y, Akbulut S, Aksungur Z, Erdemli ME, Ozhan O, Parlakpinar H. Protective effect of dexpanthenol against cisplatin-induced hepatotoxicity. *Exp Ther Med* 2018; 16: 4049-4057.
38. Rzczycki P, Yoon GS, Keswani RK, Sud S, Baik J, Murashov MD. An expandable mechanopharmaceutical device (2): Drug induced granulomas maximize the cargo sequestering capacity of macrophages in the liver. *Pharm Res* 2019; 36: 1-16.
39. El Nashar EM, Alghamdi MA, Alasmari WA, Hussein M, Hamza E, Taha RI. Autophagy Promotes the Survival of Adipose Mesenchymal Stem/Stromal Cells and Enhances Their Therapeutic Effects in Cisplatin-Induced Liver Injury *via* Modulating TGF- $\beta$ 1/Smad and PI3K/AKT Signaling Pathways. *Cells* 2021; 10: 2475.
40. Xu H, Wang Q, Fan G. The antiproliferative and antifibrotic effects of cisplatin on primary human vocal fold fibroblasts. *ORL J Otorhinolaryngol Relat Spec* 2020; 82: 188-200.

**\*Correspondence to:**

Hani M. Abdelsalam  
 Department of Zoology  
 Zagazig University  
 Zagazig  
 Egypt